scientific report

Maturation of flaviviruses starts from one or more icosahedrally independent nucleation centres

Pavel Plevka[1], Anthony J. Battisti[1], Jiraphan Junjhon[1,2], Dennis C. Winkler[3], Heather A. Holdaway[1†], Poonsook Keelapang[4], Nopporn Sittisombut[2,4], Richard J. Kuhn[1], Alasdair C. Steven[3] & Michael G. Rossmann[1+]

[1]Department of Biological Sciences, Purdue University, West Lafayette, Indiana, USA, [2]Medical Biotechnology Research Unit, National Center for Genetic Engineering and Biotechnology, National Science and Technology Development Agency, Bangkok, Thailand, [3]Laboratory of Structural Biology Research, National Institute for Arthritis, Musculoskeletal and Skin Diseases, National Institutes of Health, Bethesda, Maryland, USA, and [4]Department of Microbiology, Faculty of Medicine, Chiang Mai University, Chiang Mai, Thailand

Flaviviruses assemble as fusion-incompetent immature particles and subsequently undergo conformational change leading to release of infectious virions. Flavivirus infections also produce combined 'mosaic' particles. Here, using cryo-electron tomography, we report that mosaic particles of dengue virus type 2 had glycoproteins organized into two regions of mature and immature structure. Furthermore, particles of a maturation-deficient mutant had their glycoproteins organized into two regions of immature structure with mismatching icosahedral symmetries. It is therefore apparent that the maturation-related reorganization of the flavivirus glycoproteins is not synchronized across the whole virion, but is initiated from one or more nucleation centres. Similar deviation from icosahedral symmetry might be relevant to the asymmetrical mode of genome packaging and cell entry of other viruses.

[1]Department of Biological Sciences, 240 South Martin Jischke Drive, Purdue University, West Lafayette, Indiana 47907-2032, USA
[2]Medical Biotechnology Research Unit, c/o Medical Molecular Biology Division, Office for Research and Development, 12th Floor, Adulyadej Vikrom, Siriraj Hospital, Faculty of Medicine, National Center for Genetic Engineering and Biotechnology, National Science and Technology Development Agency, Mahidol University, Prannok, Bangkok 10700, Thailand
[3]Laboratory of Structural Biology Research, 9000 Rockville Pike, Building 50, Room 1505, National Institute for Arthritis, Musculoskeletal and Skin Diseases, National Institutes of Health, Bethesda, Maryland 20892, USA
[4]Department of Microbiology, Faculty of Medicine, Chiang Mai University, 110 Intrawaroros Road, T. Sripoom, A. Mueng Chiang Mai, Chiang Mai 50200, Thailand
[†]Present address: Case Western Reserve University, Cleveland Center for Membrane and Structural Biology, Room 111G, 1819 East 101st Street, Cleveland, Ohio 44106, USA
[+]Corresponding author. Tel: +1 765 494 4911; Fax: +1 765 496 1189; E-mail: mr@purdue.edu

INTRODUCTION

Dengue virus is a member of the *Flaviviridae* family of icosahedral, lipid-enveloped viruses, many of which are human pathogens. It is transmitted by mosquitoes and can cause haemorrhagic fever or dengue shock syndrome. During the infection process, the genomic RNA of flaviviruses replicates in the cytoplasm and then associates with the capsid protein. The nucleocapsids bud through the lipid bilayer into the lumen of the endoplasmic reticulum and, during this process, acquire the viral membrane-anchored envelope and precursor-membrane (prM) glycoproteins. The newly assembled, immature particles have a spiky surface that is formed from trimeric protrusions of the heterodimers of the envelope and prM (Zhang *et al*, 2003). The arrangement of the viral glycoproteins changes into a smooth, low pH-immature organization with a herringbone pattern as the particles pass through a low-pH environment in the *trans*-Golgi network (TGN; Zhang *et al*, 2007; Yu *et al*, 2008). The prM protein can be cleaved by furin, a host protease, into precursor and membrane fragments only after the low-pH-induced conformational change has occurred. The precursor protein dissociates from the particles when they are released into the extracellular space at neutral pH (Fig 1).

If the prM protein is not cleaved, the organization of the viral glycoproteins reverts to the spiky immature arrangement when the particles encounter neutral pH (Yu *et al*, 2008). Fully and partly immature particles together constitute approximately 40% of all particles in wild-type dengue virus type 2 (DENV2) preparations and the purified virus contains a fraction of intact prM molecules (van der Schaar *et al*, 2007; Junjhon *et al*, 2010). The fraction of cleaved prM protein can be further reduced by mutations in the prM protein—such as the prR201A substitution, associated with the furin cleavage site—resulting in an increased fraction of immature-like particles (particles that went through the complete maturation pathway, but their glycoprotein conformation changed into immature because of limited prM cleavage; Junjhon *et al*, 2008, 2010). Alternatively, adding NH_4Cl to the media after infection can help produce immature flavivirus particles (Yu *et al*,
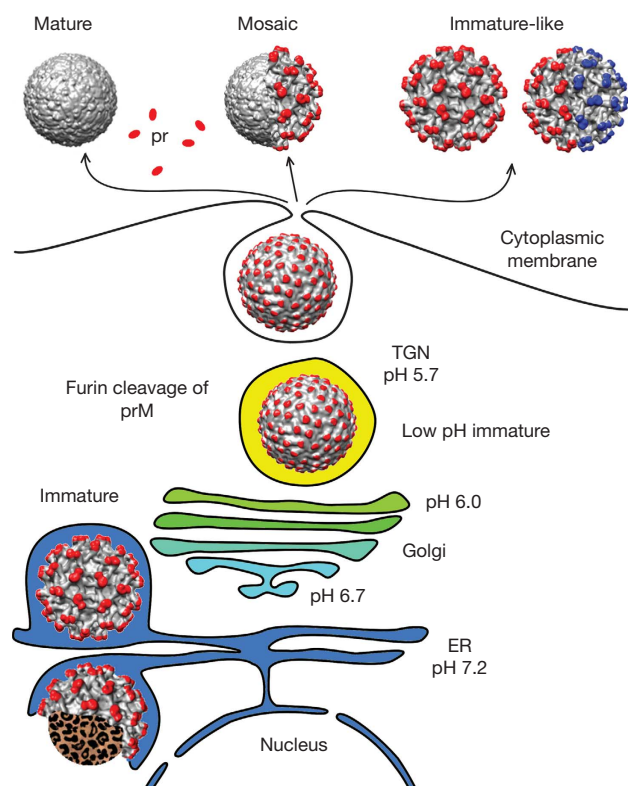
Fig 1 | A model of flavivirus maturation pathways. Immature particles form by budding into the endoplasmic reticulum. The envelopes of these particles have a single icosahedral symmetry. A conformational change of the virion occurs as the particles are transported to the acidic pH in the Golgi and TGN. The prM protein can be cleaved by the host protease furin after the conformational change, but not all prM molecules are cleaved. Depending on the fraction of prM cleaved, the particles might adopt mature, mosaic or immature-like conformations when released from cells. The cleaved precursor proteins are released from particles at neutral pH in the extracellular space. The immature-like particles only constitute approximately 3% of wild-type virions that are released from cells, but are abundant for the prM cleavage-deficient prR201A mutant. About 50% of the immature-like particles of the prR201A mutant had their envelopes organized into two regions, each of which correspond to an immature structure, but the two regions were symmetrically mismatched. The pr/prM proteins are shown in red/blue and the envelope proteins are shown in grey. The red and blue colours of prM indicate mismatched icosahedral symmetries. ER; endoplasmic reticulum; pr, precursor; prM, precursor membrane; TGN, *trans*-Golgi network.

2008). The NH_4Cl changes the pH in the TGN to neutral, preventing the maturation process. Although purified immature virions are non-infectious, they can be endocytosed upon interaction with some prM or envelope antibodies (Rodenhuis-Zybert *et al*, 2010). Subsequent cleavage of the prM in the endosome might make these particles infectious. Thus, the immature and mosaic particles (that contain both mature and immature regions) could contribute to flavivirus infection (Cherrier *et al*, 2009a; Rodenhuis-Zybert *et al*, 2010).

The structures of mature and immature particles of DENV2 and West Nile virus were determined previously by single-particle
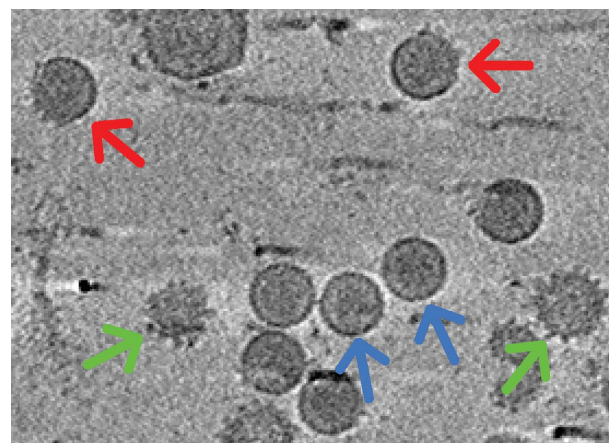
Fig 2 | Central section through a tomogram of particles produced by wild-type DENV2 infection. Mature, mosaic and immature-like particles are indicated by blue, red and green arrows, respectively. DENV2, dengue virus type 2.

cryo-electron microscopy reconstructions. Here, we report a cryo-electron tomography analysis of mosaic wild-type dengue particles and apparently fully immature particles of the prR201A mutant.

RESULTS AND DISCUSSION
Structure of mosaic particles of wild-type DENV2
Cryo-electron tomography analysis of DENV2 particles confirmed the existence of mosaic particles containing mature and immature regions (Fig 2; Nelson *et al*, 2008; Cherrier *et al*, 2009a). The structure of the immature particle has 60 prominent surface spikes, whereas the surface of the mature structure is smooth. The orientation of the icosahedral symmetry of the immature part of a mosaic particle could be identified by maximizing the correlation between the sub-tomogram and the known structure of the immature particle (Fig 3A; Zhang *et al*, 2003). Orientation of the icosahedral symmetry of the mature part of the mosaic particles could not be established in the same way because at approximately 40 Å resolution, the structure of mature dengue virus does not have any prominent features. This is shown by the high (0.96) correlation coefficient between the cryo-electron-microscopy structure of a mature particle at 40 Å resolution and a spherically averaged version of the structure. However, the two versions of the structure could be distinguished on the basis of their radial distribution of density. As the orientation of the mature part of the mosaic particles could not be established, the spherically averaged model of the mature particle was used to identify the mature parts on the mosaic particle.

To determine which regions of the mosaic particles resemble the mature or the immature structure, correlation coefficients were calculated for each volume covering an icosahedral asymmetric unit between the two known structures and the particle in the sub-tomogram. Mosaic particles were found to have their glyco-proteins organized into two regions—one correlating with the mature and the other correlating with the immature structure (Fig 4). The surface areas occupied by the mature and immature regions varied among the 14 mosaic particles analysed. There was a border zone between the two regions that correlated poorly with both mature and immature structures. The width of the border
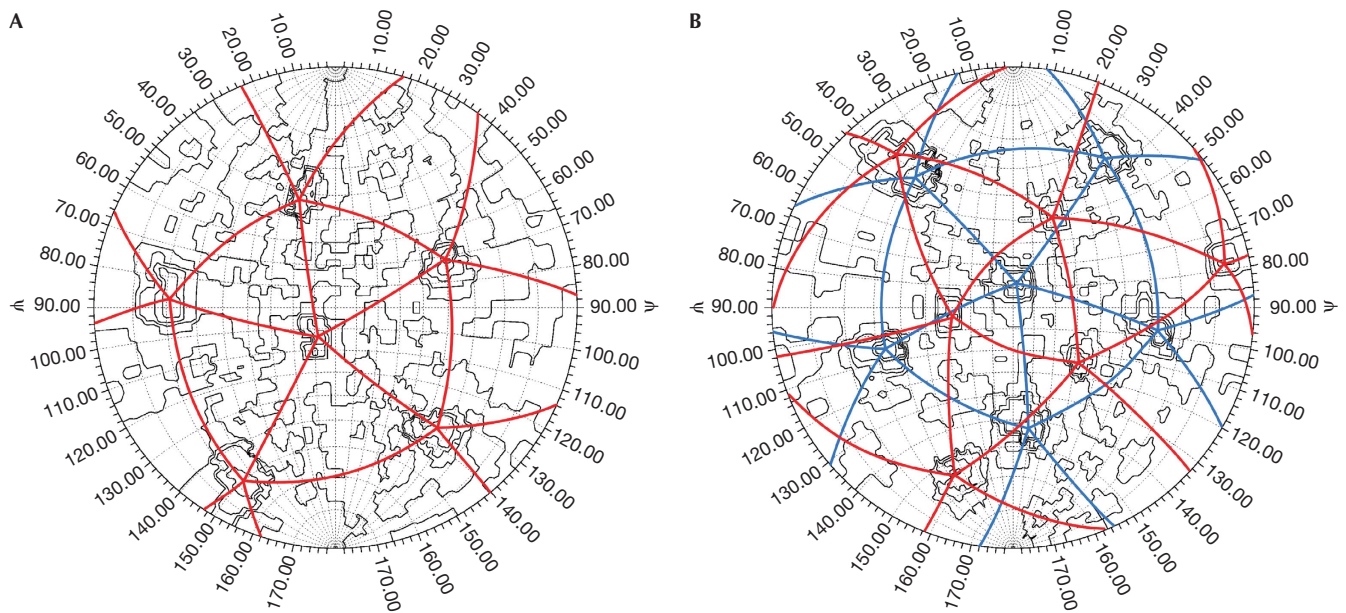
Fig 3 | Cross-correlation searches to determine the orientation of particles in the sub-tomograms. Model particles in different orientations were compared with particles in the sub-tomograms and the resulting correlation coefficients were plotted on a stereographic projection (the plots are analogous to the representation of the surface of the Earth onto a flat map). See Methods section for details. **(A)** Comparison of the wild-type mosaic particle sub-tomogram with the immature dengue virus structure. **(B)** Comparison of the prR201A mutant immature-like particle with the immature dengue virus structure. Peaks in the searches correspond to positions of fivefold symmetry axes in the tomograms (see Methods section for details). The interval between contours is 1σ. The coloured lines connect the icosahedral fivefold symmetry axes. The search in **(B)** shows peaks corresponding to two independent icosahedral symmetries.
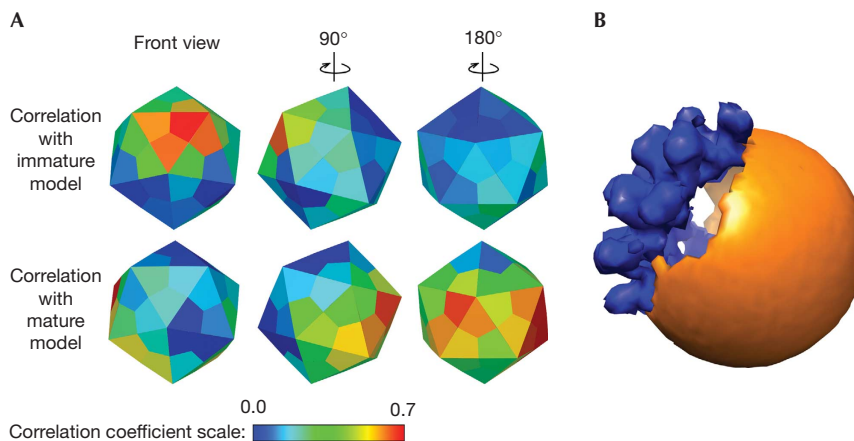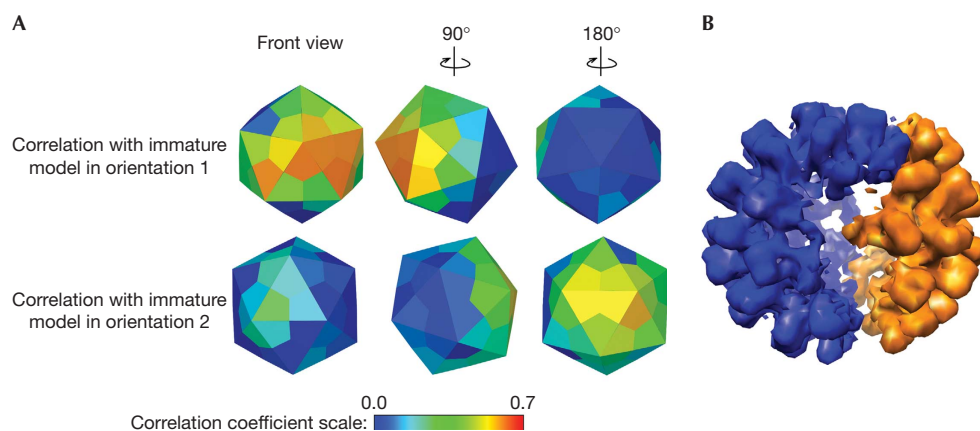

Fig 4 | Structural analysis of a dengue virus type 2 mosaic particle. (A) The colours of the icosahedral faces represent the correlation coefficient for a particular icosahedral asymmetrical unit, compared with immature (upper row) and mature (bottom row) dengue virus structures. The icosahedral symmetry of the mature part of the particle is shown to be coincident with the symmetry of the immature part, but this could not be experimentally verified. **(B)** Model of the mosaic particle. Regions that had higher than 0.25 correlation with the immature structure are shown as an immature structure in blue. Regions that had higher than 0.25 correlations with the mature structure are shown as a spherical orange surface.

zone was roughly that of one icosahedral asymmetric unit. The high correlation beween the mature and immature regions and their respective models indicate that even glycoproteins close to each other can have different, but functionally relevant, conformations and might perform different functions in the life-cycle of the virus.

Disruption of global icosahedral symmetry
Preparations of DENV2 contain only approximately 3% of completely immature-like particles (Junjhon *et al*, 2008). Thus,

the prR201A mutant, which has lower prM cleavage efficiency (approximately 50% of the particles produced by this mutant are immature-like; the remainder are mosaic or mature), was used to analyse immature-like particles. Two independent orientations of icosahedral symmetry were found in 14 of the 30 immature-like particles analysed. The glycoprotein envelope of these particles was organized into two exclusive regions (Fig 3B). Within each region, the glycoprotein arrangement resembled that of the immature particle, but the two regions did not coherently fit

Fig 5 | Structural analysis of the dengue virus type 2 prR201A mutant immature-like particle. (**A**) The colours of the icosahedral faces represent the correlation coefficient for a particular icosahedral asymmetrical unit compared with the immature dengue virus structure in one of the two alternative orientations. The orientations of icosahedrons in the top and bottom rows show the relative orientations of the icosahedral symmetries of the two regions. (**B**) Model of the immature particle with double symmetry. Regions that had higher than 0.25 correlation with the immature structure in orientation 1 are shown in blue. Similarly, regions that had higher than 0.25 correlations with the immature structure in orientation 2 are shown in orange.

together in a single icosahedral lattice (Fig 5). As in the mosaic particles described above, the border zone between the two regions was about one icosahedral asymmetrical unit wide. The relative size of the two regions varied between particles. Particles with more than two regions of unrelated icosahedral symmetry were not observed. It is nevertheless possible that small patches of icosahedrally ordered particle envelope were missed due to the limited sensitivity of the orientation search. Similar experiments on wild-type immature virus produced in cells grown in the presence of 20 mM NH_4Cl showed only a single icosahedral symmetry for each particle (data not shown).

The immature-like particles that were released from infected cells passed through the TGN, where their glycoproteins changed conformation to the low-pH immature state. As most of their prM protein was probably not cleaved (Junjhon et al, 2008), the particles reverted to an immature-like state after being released to the extracellular space at neutral pH (Fig 1). As 'double symmetry' was not observed in immature DENV particles produced from cells grown in the presence of NH_4Cl, it is likely that the double symmetry in the R201A-mutant particles originated during the reversion from the low-pH immature conformation to the neutral-pH immature form. As the R201A mutation does not completely prevent the furin cleavage, it is possible that the border regions in the double symmetry particles contained cleaved precursor proteins and contributed to the mismatch of symmetry.

The glycoprotein envelope of an immature flavivirus particle consists of 60 spikes. Each spike is a trimer of envelope-prM heterodimers. Maturation of flavivirus virions requires large conformational changes and re-assortment of the 60 trimers of heterodimers into 90 dimers of heterodimers (Yu et al, 2008). When the low-pH immature structure reverts to the neutral-pH immature structure, the heterodimers from a given spike might revert to their original configuration, or the spikes might be formed by different sets of heterodimers. If the same spikes as were in the original, immature particle are reformed, the resulting particle will have a single coherent icosahedral symmetry. Conversely, if the heterodimers are redistributed, two local icosahedral symmetries

on a single particle could occur if the reorganization starts from two incompatible nucleation centres. As the two centres of immature organization propagate around the particle (in the manner of falling domino pieces), the two immature regions might encounter each other in an arrangement that does not allow the whole particle to be united into a single global icosahedral symmetry. Whereas the initial virion assembly results in production of icosahedrally symmetrical immature particles, the re-assortment of the glycoproteins within one particle might be a chain reaction initiated from one or a few nucleation centres.

Almost all structural analyses of icosahedral particles so far have been on the basis of averages. The many crystallographic investigations of viruses in the last 30 years (Rossmann & Johnson, 1989; Liljas, 1999; Johnson & Chiu, 2000) depend on the dominant icosahedral symmetry, usually established by calculation of a rotation function (Rossmann & Blow, 1962). The crystallization process can be a screen for excluding particles with several symmetries. If some of the particles with imperfect symmetry had been incorporated into a crystal consisting primarily of icosahedral particles, the presence of particles with aberrant symmetry would not have been apparent. Similarly, in most cryo-electron-microscopy analyses of icosahedral viruses (Baker et al, 1999), icosahedral symmetry is assumed during the reconstruction. If any of the particles have regions with mismatched icosahedral symmetry, they would probably be rejected during the reconstruction process. The results presented here are among the first to examine the symmetry of individual particles. The occurrence of some degree of breakdown in icosahedral symmetry should not be surprising in view of the singular portal vertices of tailed bacteriophages and even of large icosahedral phages, such as PBCV-1 and Mimiviruses (Xiao et al, 2009; Cherrier et al, 2009b). Furthermore, the small icosahedral parvoviruses have been shown to have an asymmetrical receptor-binding site (Hafenstein et al, 2007). In the present case, the occurrence of two icosahedral symmetries in the same particle seems to be the result of incomplete maturation and subsequent reversal of the virus to an immature-like form. The presence of

asymmetry in phages, or in Chlorella viruses such as PBCV-1, is clearly an evolutionarily selected advantage. The benefits of the asymmetry for flaviviruses remain to be established.

METHODS

Specimen preparation. Wild-type DENV2 16681 and the DENV2 16681 R201A mutant were produced and purified as described previously (Junjhon *et al*, 2008; Yu *et al*, 2008). The virus solutions were mixed with a suspension of 10 nm colloidal gold particles. The mixed solution (3.5 µl) was applied to a holey carbon film, blotted, and vitrified by plunging into liquid ethane to prepare the sample for cryo-electron microscopy.

Cryo-electron microscopy. Tilt series of the prR201A DENV2 mutant were obtained using a Philips (Andover, MA, USA) CM300 or FEI (Hillsboro, OR, USA) Titan Krios electron microscope operated at 300 keV. The Krios microscope was equipped with a Gatan (Pleasanton, CA, USA) energy filter that was operated in the zero-energy-loss mode with a slit width of 30 e−V. Images were recorded on a 2,048 × 2,048-pixel charge-coupled device (CCD) camera at a nominal magnification of 19,500 at 7 µm defocus. Tilt series of immature and mature wild-type DENV2 virus were collected on a Tecnai-12 electron microscope (FEI, Hillsboro, OR, USA) operated at 120 keV. The microscope was equipped with a Gatan GIF 2002 energy filter that was operated in the zero-energy-loss mode with a slit width of 20 e−V. Images were recorded on a 2,048 × 2,048-pixel CCD camera (Gatan, Pleasanton, CA, USA) at a nominal magnification of 16,500 at 3–5 µm defocus. All tilt series were obtained using a 2 ° angular increment and ranged from approximately −64 ° to 64 °. The cumulative electron doses were approximately 85 e−/Å^2.

Image processing. Tomograms were calculated from tilt series using IMOD (Kremer *et al*, 1996). The final analyses were performed on 2 × binned tomograms with a voxel size of 15.6 Å. Sub-tomograms of 50 × 50 × 50 voxels, containing an image of a virus, were excised. Particles were contrast inverted and roughly centred with Proc3d (Ludtke *et al*, 1999).

Sub-tomogram analysis. The orientation of a particle in a sub-tomogram was determined by finding the highest correlation coefficient between the particle in the sub-tomogram and a series of differently oriented structures of immature DENV2 derived from a single-particle cryo-electron-microscopy reconstruction (Yu *et al*, 2008). As the model had icosahedral symmetry, the resultant plot of the rotation search also had icosahedral symmetry. The model was superimposed onto the observed tomogram with one of the fivefold axes of the model along a direction defined by polar angles ψ and φ (Rossmann & Blow, 1962) in the observed tomogram. The model was then compared with the tomogram in a series of rotations about the defined axis in increments of $\kappa = 2.5$ °. The highest correlation coefficient, comparing the density distribution of the model and the tomogram, was then selected from this series and plotted onto a stereographic projection. Combinations of the ψ and φ angles were explored in increments of approximately 2.5 °. The orientations corresponding to the highest correlation coefficient and position of particle centre were then refined with smaller angular and translational increments, respectively.

Resolution of the tomograms. A Fourier shell correlation between the icosahedrally averaged sub-tomogram and the 9 Å cryo-electron microscopy single-particle reconstruction fell below 0.5 at 40 Å resolution.

CONFLICT OF INTEREST

The authors declare that they have no conflict of interest.

REFERENCES

Baker TS, Olson NH, Fuller SD (1999) Adding the third dimension to virus life cycles: three-dimensional reconstruction of icosahedral viruses from cryo-electron micrographs. *Microbiol Mol Biol Rev* **63:** 862–922

Cherrier MV *et al* (2009a) Structural basis for the preferential recognition of immature flaviviruses by a fusion-loop antibody. *EMBO J* **28:** 3269–3276

Cherrier MV, Kostyuchenko VA, Xiao C, Bowman VD, Battisti AJ, Yan X, Chipman PR, Baker TS, Van Etten JL, Rossmann MG (2009b) An icosahedral algal virus has a complex unique vertex decorated with a spike. *Proc Natl Acad Sci USA* **106:** 11085–11089

Hafenstein S *et al* (2007) Asymmetric binding of transferrin receptor to parvovirus capsids. *Proc Natl Acad Sci USA* **104:** 6585–6589

Johnson JE, Chiu W (2000) Structures of virus and virus-like particles. *Curr Opin Struct Biol* **10:** 229–235

Junjhon J *et al* (2008) Differential modulation of prM cleavage, extracellular particle distribution, and virus infectivity by conserved residues at nonfurin consensus positions of the dengue virus pr-M junction. *J Virol* **82:** 10776–10791

Junjhon J *et al* (2010) Influence of pr-M cleavage on the heterogeneity of extracellular dengue virus particles. *J Virol* **84:** 8353–8358

Kremer JR, Mastronarde DN, McIntosh JR (1996) Computer visualization of three-dimensional image data using IMOD. *J Struct Biol* **116:** 71–76

Liljas L (1999) Virus assembly. *Curr Opin Struct Biol* **9:** 129–134

Ludtke SJ, Baldwin PR, Chiu W (1999) EMAN: semiautomated software for high-resolution single-particle reconstructions. *J Struct Biol* **128:** 82–97

Nelson S *et al* (2008) Maturation of West Nile virus modulates sensitivity to antibody-mediated neutralization. *PLoS Pathog* **4:** e1000060

Rodenhuis-Zybert IA, van der Schaar HM, Silva Voorham JM, Ende-Metselaar H, Lei HY, Wilschut J, Smit JM (2010) Immature dengue virus: a veiled pathogen? *PLoS Pathog* **6:** e1000718

Rossmann MG, Blow DM (1962) The detection of sub-units within the crystallographic asymmetric unit. *Acta Crystallogr* **15:** 24–31

Rossmann MG, Johnson JE (1989) Icosahedral RNA virus structure. *Annu Rev Biochem* **58:** 533–573

van der Schaar HM, Rust MJ, Waarts B-L, van der Ende-Metselaar H, Kuhn RJ, Wilschut J, Zhuang X, Smit JM (2007) Characterization of the early events in dengue virus cell entry by biochemical assays and single-virus tracking. *J Virol* **81:** 12019–12028

Xiao C, Kuznetsov YG, Sun S, Hafenstein SL, Kostyuchenko VA, Chipman PR, Suzan-Monti M, Raoult D, McPherson A, Rossmann MG (2009) Structural studies of the giant Mimivirus. *PLoS Biol* **7:** e1000092

Yu I-M, Zhang W, Holdaway HA, Li L, Kostyuchenko VA, Chipman PR, Kuhn RJ, Rossmann MG, Chen J (2008) Structure of the immature dengue virus at low pH primes proteolytic maturation. *Science* **319:** 1834–1837

Zhang Y, Corver J, Chipman PR, Zhang W, Pletnev SV, Sedlak D, Baker TS, Strauss JH, Kuhn RJ, Rossmann MG (2003) Structures of immature flavivirus particles. *EMBO J* **22:** 2604–2613

Zhang Y, Kaufmann B, Chipman PR, Kuhn RJ, Rossmann MG (2007) Structure of immature West Nile virus particles. *J Virol* **81:** 6141–6145